First-order phase transition between dimerized-antiferromagnetic and uniform-antiferromagnetic phases in $Cu_{1-x}M_xGeO_3$

T. Masuda,[*][†] I. Tsukada,[‡] and K. Uchinokura[†]

Department of Applied Physics, The University of Tokyo, 6th Engineering Building, 7-3-1 Hongo, Bunkyo-ku, Tokyo 113-8656, Japan

Y. J. Wang, V. Kiryukhin, and R. J. Birgeneau

Department of Physics, Massachusetts Institute of Technology, Cambridge, Massachusetts 02139

(Received 8 June 1999)

We have performed detailed magnetic susceptibility measurements as well as synchrotron x-ray-diffraction studies to determine the temperature vs concentration (T-x) phase diagram of $Cu_{1-x}Mg_xGeO_3$. We observe clear double peaks in the magnetic susceptibility implying two antiferromagnetic (AF) transition temperatures in samples with Mg concentrations in the range $0.0237 \leq x \leq 0.0271$. We also observe a drastic change in the inverse correlation length in this concentration range by x-ray diffraction. The drastic change of the AF transition temperature as well as the disappearance of the spin-Peierls phase have been clarified; these results are consistent with a first-order phase transition between dimerized AF and uniform AF phases as reported by T. Masuda *et al.* [Phys. Rev. Lett. **80**, 4566 (1998)]. The T-x phase diagram of $Cu_{1-x}Zn_xGeO_3$ is similar to that of $Cu_{1-x}Mg_xGeO_3$, which suggests that the present phase transition is universal for $Cu_{1-x}M_xGeO_3$.

I. INTRODUCTION

The discovery of the inorganic spin-Peierls (SP) cuprate $CuGeO_3$ (Ref. 1) has made it possible to study systematically the effect of impurities on SP systems. The effect of substitution of $Zn^{2+}(S=0)$ for Cu^{2+} was studied by Hase *et al.*[2] and the appearance of an antiferromagnetic (AF) phase at temperatures below the SP transition temperature (T_{SP}) was reported.[3,4] Both dimerization superlattice and AF magnetic peaks were observed by neutron-diffraction measurements below the AF transition temperature (T_N) (Refs. 5–7); the coexistence of these two seemingly exclusive order parameters was explained theoretically by using a phase Hamiltonian method.[8] Recently, some of the present authors studied the transition temperature vs impurity concentration (T-x) phase diagram in $Mg^{2+}(S=0)$-doped $CuGeO_3$ by means of dc susceptibility measurements.[9] These authors observed the disappearance of the cusp due to the SP transition and the sudden increase of the AF transition temperature at an impurity concentration $x=x_c \sim 0.023$. They therefore concluded that there was a first-order phase transition between dimerized-antiferromagnetic (DAF) and uniform-antiferromagnetic (UAF) phases. The disappearance of the long-range order (LRO) of the dimerization above a critical impurity concentration was tentatively explained theoretically as a second-order phase transition at $T=0$ K.[10] In this paper we report detailed studies on the temperature dependence of the magnetic susceptibility and, consequently, the T-x phase diagram of $Cu_{1-x}M_xGeO_3$ ($M=$ Mg and Zn) near $x \sim 0.024$ (Mg) and 0.020 (Zn). We have obtained clear evidence for a first-order phase transition between UAF and DAF phases in these nonmagnetic impurity-doped systems thereby strengthening the conclusion of the previous work.[9] We have also used high-resolution synchrotron x-ray-diffraction techniques to clarify the SP phase region in the phase diagram. As a result we have confirmed the disappearance of the SP-LRO at $x \gtrsim x_c$. More importantly, we have found that the SP correlation length for a given x becomes long range at a lower temperature[11] (T'_{SP}) than the SP transition temperature previously reported and T'_{SP} crosses the antiferromagnetic phase boundary at $x \sim 0.024$; this gives a phenomenological explanation for the origin of the putative first-order phase transition.

II. EXPERIMENTAL DETAILS

All the samples were high quality single crystals grown by the floating-zone (FZ) method; the concentration of the Mg^{2+} or Zn^{2+} dilutant x was determined by inductively coupled plasma atomic emission spectroscopy (ICP-AES). To determine the phase boundary we paid special attention to any possible inhomogeneity of the impurity concentration. We show a rough sketch of typical bulk single crystals of $Cu_{1-x}M_xGeO_3$ ($M=$ Mg and Zn) in Fig. 1. The crystals were grown by using small pure or slightly doped $CuGeO_3$ single crystals as the seed crystals. When the seed crystal contains a smaller concentration than that of starting polycrystalline material, the actual grown crystal rod has a concentration gradient at the end corresponding to the initial growth stage and then the concentration saturate at the later growth stage. For the measurements of physical properties we used parts of the crystals in the saturated region, so that the concentration distribution along the c direction of the samples we have studied is within the inhomogeneity along the radial direction. We estimated the accuracy of the impurity concentration from the fluctuation of the saturated concentration in a few of the rods. From this we concluded that any errors in the concentration are within 0.1% in $Cu_{1-x}Mg_xGeO_3$ and 0.3% in $Cu_{1-x}Zn_xGeO_3$ in the region of $0.02 < x < 0.03$. It is apparent that Mg-doped $CuGeO_3$ is preferable to Zn-doped $CuGeO_3$ for studies of impurity effects because of the more accurate control of x. The use of

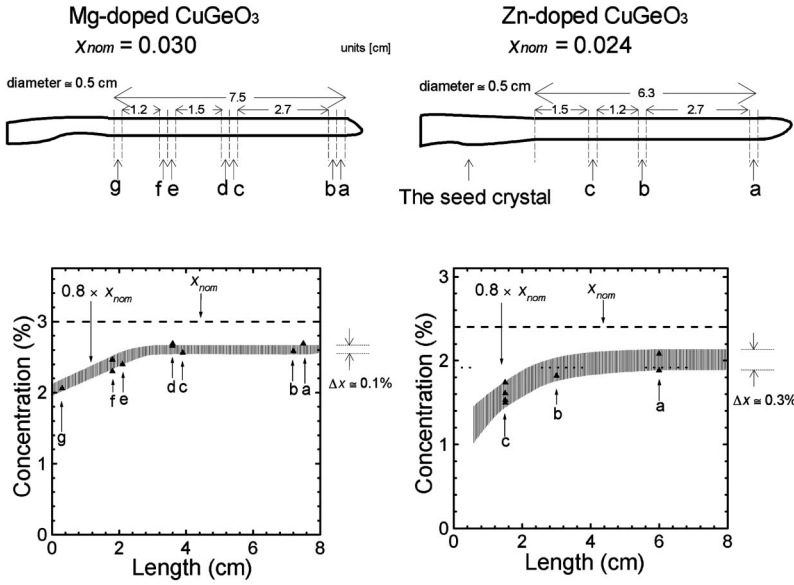FIG. 1. Sketches of bulk single crystals of $Cu_{1-x}M_xGeO_3$ ($M = Mg$ and Zn) grown by the FZ method. In some cases we analyzed more than one piece. The figures in the bottom show the concentration determined by ICP-AES vs crystal-growth length.

Mg^{2+} as a dilutant made it possible to observe unambiguously the phase transition between the DAF and UAF phases in impurity-doped $CuGeO_3$.[9] Careful treatment of Zn^{2+}-doped samples also have made a similar observation possible in the present study.

Measurements of the dc magnetic susceptibility were performed with a commercial super conducting quantum interference device magnetometer (χ-MAG, Conductus Co., Ltd.). The synchrotron x-ray-diffraction measurements were carried out at the MIT-IBM beamline X20A at the National Synchrotron Light Source (NSLS), Brookhaven National Laboratory.[11]

III. EXPERIMENTAL RESULTS

The magnetic susceptibility in an applied field parallel to the c axis $[\chi_c(T)]$ in $Cu_{1-x}Mg_xGeO_3$ samples around x_c in the region of $2 < T < 5$ K is shown in Fig. 2(a). We observe clear double peaks in samples whose x's are 0.0237, 0.0248, 0.0254, and 0.0271, while only one sharp peak is observed in 0.0229 and 0.0288 samples. In contrast to the previous measurements,[9] we took the data using temperature steps of 0.025 K; this reveals the detailed behavior of the susceptibility around $x \sim x_c$. The inset in the bottom of Fig. 2(a) shows $\chi_c(T)$ over a wider temperature range. One can see the disappearance of the cusp in $\chi_c(T)$ around 10 K in the $x = 0.0288$ sample while the cusp exists in the $x = 0.0271$ sample. This suggests that the SP transition still exists in the $x = 0.0271$ sample and disappears in the $x = 0.0288$ sample. Here we define x_{c1} as the concentration x where the double peaks first begin to appear, and x_{c2} as the concentration x, where only one peak begins to be observed and at the same time the cusp in $\chi_c(T)$ corresponding to T_{SP} disappears, with increasing x. With these definitions, we obtain $x_{c1} = 0.0237$ and $x_{c2} = 0.0271$. In cases when we do not distinguish x_{c1} and x_{c2}, we use simply x_c, hereafter. We determined T_{SP} from the crossing points of linear functions fitted to $\chi_c(T)$ above and below the putative transition. We adopted Fisher's theory[12] to determine the AF transition temperature, according to which the AF transition temperature is

signalled by a maximum in $\partial(\chi_\| T)/\partial T$. When there are two peaks in $\partial(\chi_\| T)/\partial T$, we define T_{N1} and T_{N2} as the maxima at lower and higher temperatures, respectively [see the inset in the upper left of Fig. 2(a)]. If there is only one peak, we define the Néel temperature simply as T_N. In this way we obtained the T-x phase diagram of $Cu_{1-x}Mg_xGeO_3$ near x_c shown in Fig. 2(b).

In Ref. 9 the existence of a first-order phase transition between the DAF and UAF phases was inferred from the observation of a sudden increase of T_N at $x = 0.023$, the broadening of $\chi_c(T)$ around T_N, and the disappearance of the cusp due to the SP transition. Instead of a single broad peak, we now observe clear double peaks. T_N below x_{c1} is smoothly connected to T_{N1} at x_{c1}, while T_{N2} is smoothly connected to $T_N(x > x_{c2})$ at x_{c2}. Therefore T_{N1} and T_{N2} may be confidently assigned as the AF transition temperatures with respect to the DAF and UAF phases, respectively. The lower T_N curve never joins with the higher T_N curve, which shows more directly the presence of the proposed first-order phase transition. Note that the double peaks are observed in the finite concentration region, $x_{c1} < x < x_{c2}$, where the lower and upper boundaries are separated in x by amounts well above our resolution of concentration.

The phase transition between the DAF and UAF phases was also verified in neutron-diffraction experiments.[13] Nakao *et al.*[13] determined x_c as ~ 0.027 by the observation of a peak of the effective magnetic moment and the jump of the magnitude of dimerization. This value is approximately equal to x_{c2} of the present paper. On the other hand, from the magnetic susceptibility measurements x_c was deduced to be about 0.023.[9] To determine at what temperature true SP-LRO is attained, synchrotron x-ray diffraction is a superior technique to neutron diffraction, because of its naturally very high resolution (~ 0.0002 Å^{-1}). The peak profiles of longitudinal scans at (1.5, 1, 1.5) of samples with $x = 0.021$ and 0.026 are shown in the inset of Fig. 2(c). We observe superlattice peak in the samples with $x \geq 0.023$ but the peak width is far wider than the resolution limit (5000 Å) even at low temperatures, that is, we determine that only SP-SRO exists in these samples. The concentration dependence of the in-

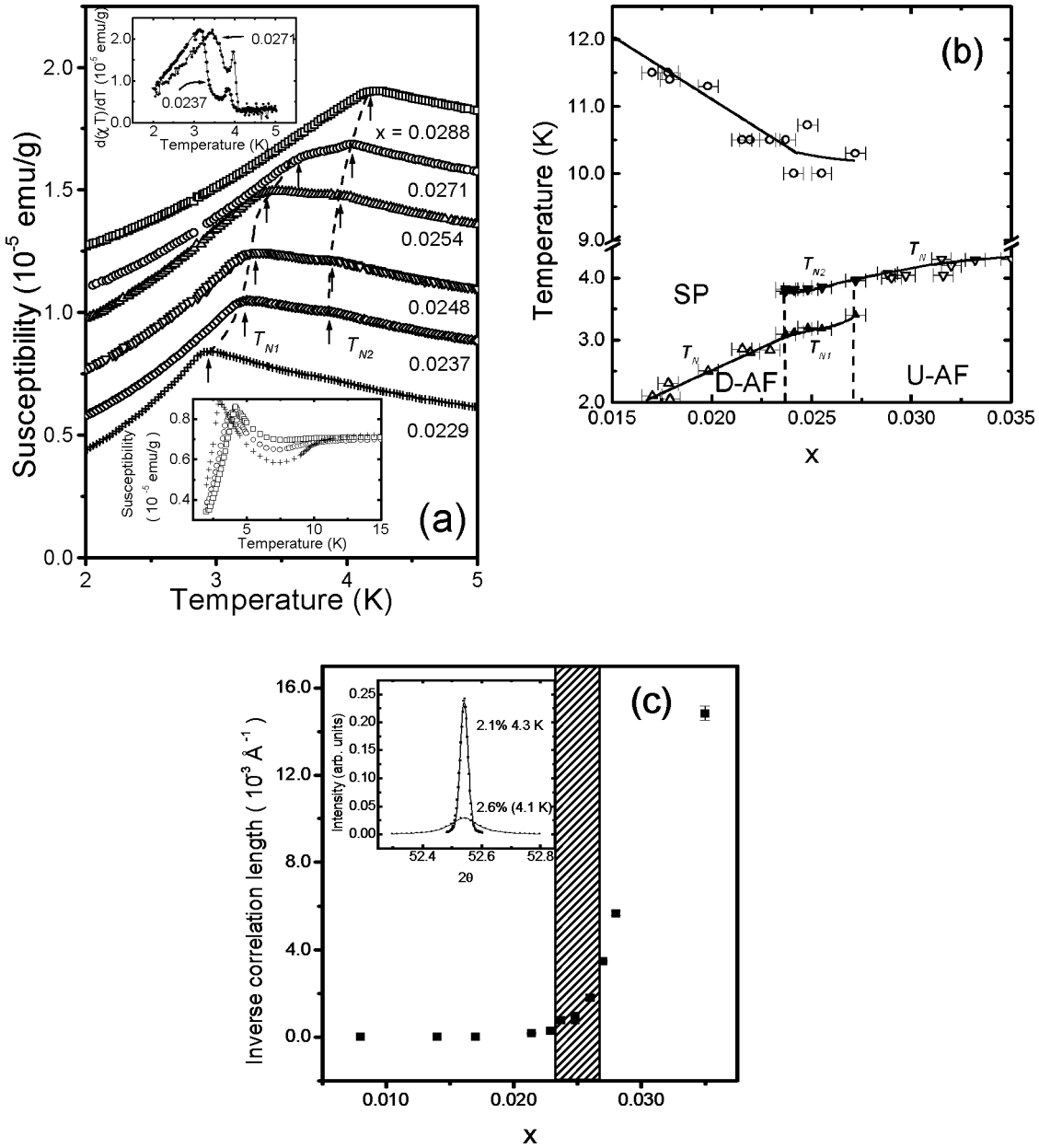FIG. 2. (a) The magnetic susceptibility of $Cu_{1-x}Mg_xGeO_3$ near the AF transition temperature(s). The applied field is 1000 Oe. The data for different x are shifted vertically. Double peaks are observed in the region of $0.0237 \leq x \leq 0.0271$, while a single peak is observed in the regions of $x < 0.023$ and $0.028 > x$. The arrows indicate the anomaly due to the AF transition. The inset in the upper left is $\partial(\chi_\parallel T)/\partial T$ for determining T_{N1} and T_{N2}. The inset in the bottom shows the magnetic susceptibility in the same samples of $x = 0.0271$, 0.0288, and 0.0299 for $2 < T < 15$ K. (b) The temperature vs concentration phase diagram determined by the magnetic susceptibility measurements. Open circles, triangles, closed upward and downward triangles are T_{SP}, T_N, T_{N1}, and T_{N2}, respectively. Solid lines are guides to the eye. (c) Mg concentration dependence of the inverse correlation length of the lattice dimerization at $T = 4$ K. The inset shows representative superlattice peak profiles.

verse correlation length at 4 K is shown in Fig. 2(c). The hatched zone corresponds to the double-peak region of the DAF and UAF phases determined by the magnetic susceptibility measurements. The correlation length (ξ) is larger than the resolution limit of 5000 Å at low temperatures for $x < x_{c1}$, decreases drastically in the double peak region, and becomes much shorter at $x > x_{c2}$.

We now discuss the Zn-doped $CuGeO_3$ system. As one might expect, the phase transition between the DAF and UAF phases exists not only in the case of Mg-doped

$CuGeO_3$ but also in Zn-doped $CuGeO_3$. $\chi_c(T)$ of $Cu_{1-x}Zn_xGeO_3$ ($x = 0.016$, 0.017, 0.019, 0.023, and 0.025) in the region of $2 < T < 5$ K is shown in Fig. 3. Again we observe double peaks in samples with Zn^{2+} concentrations of $x = 0.017$, 0.019, and 0.023, while a single peak is observed in the $x = 0.016$ and 0.025 samples; generally, the peak structure is not as clear as that of $Cu_{1-x}Mg_xGeO_3$. $\partial(\chi_\parallel T)/\partial T$ is shown in the inset in the upper left. The ambiguity seems to be due to the worse dilutant homogeneity in the Zn-doped samples compared with that of the Mg-doped
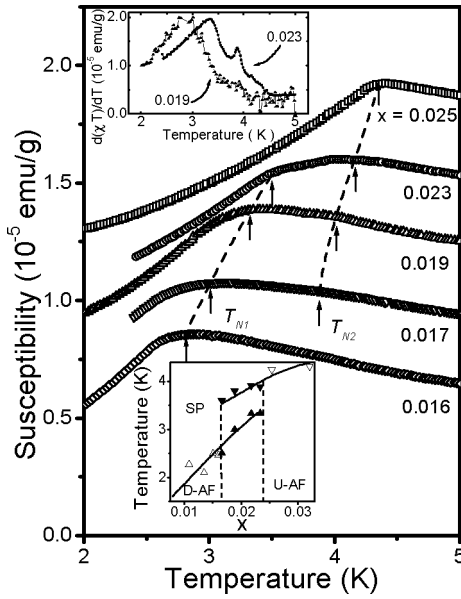
FIG. 3. The magnetic susceptibility of $Cu_{1-x}Zn_xGeO_3$ around T_N. Double peaks are observed in $x=0.019$, and 0.023 samples, while single peaks are observed in $x=0.016$ and 0.025 samples. In $x=0.017$ the anomaly at T_{N2} is confirmed by Fisher's method though it is not so clear in the raw susceptibility data. The inset in the bottom shows the T-x phase diagram. The inset in the upper left is $\partial(\chi_\parallel T)/\partial T$.

samples as we explained in the previous section. In the case of Zn-doped $CuGeO_3$ we obtain $x_{c1} \simeq 0.017$ and $x_{c2} \simeq 0.023$. The T-x phase diagram near x_c is shown in the inset in the bottom. We observe a jump of T_N in Zn-doped $CuGeO_3$ which is closely analogous to that in Mg-doped $CuGeO_3$.

Now let us return to the SP transition in the Mg-doped $CuGeO_3$ system. Figures 4(a) and (b) show the experimental results of the magnetic susceptibility measurement and the heat-capacity measurement of $Cu_{1-x}Mg_xGeO_3$ ($x=0.017$). We observe a cusp due to the SP transition at $T \sim 11.5$ K in the magnetic susceptibility [Fig. 4(a)]. As for heat capacity, we observe an anomaly due to the SP transition at $T \sim 10.7$ K [Fig. 4(b)]. From neutron-diffraction measurements on the same concentration sample, it is found that the superlattice peak intensity begins to increase at $T \sim 10.8$ K in Fig. 2 of Ref. 13. The coincidence of these temperatures is good enough, and thus we concluded that T_{SP} of the sample is about 11 K.

On the other hand, high-resolution x-ray-diffraction measurements lead to rather different conclusions. We observe that the peak width of the superlattice reflection is not resolution limited at the T_{SP} determined above but rather it continues to narrow as the temperature is lowered below T_{SP} as shown in Fig. 2 of Ref. 11. Here, we define the temperature where the SP correlations become long range as T'_{SP} and it is much lower than T_{SP}, especially for x near x_c. The length 5000 Å, corresponding to the resolution limit of the measurement, is much longer than the average impurity distance and consequently we may safely call the region of $T \lesssim T'_{SP}$ as the SP long-range order (LRO) region.

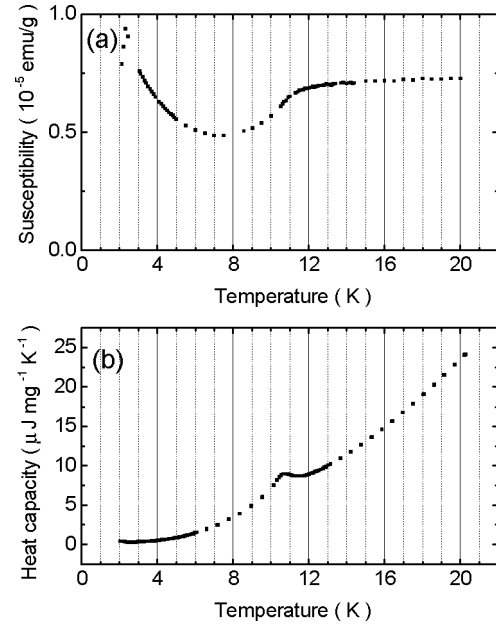Since T'_{SP} is lower than T_{SP}, true SP-LRO only exists at

FIG. 4. The experimental results of (a) the magnetic susceptibility and (b) heat capacity in $Cu_{1-x}Mg_xGeO_3$ ($x=0.017$) sample.

a temperature which is rather lower than the T_{SP} deduced from the susceptibility measurements. The difference between T_{SP} and T'_{SP} does not reflect any experimental artifact because the behavior of the x-ray integrated intensity shows almost the same temperature dependence as the peak intensity of the neutron diffraction. We should note that the resolution of neutron diffraction is much less (~ 200–500 Å),[13] and actually the peak intensity of the neutron diffraction corresponds to the integrated intensity of the x-ray diffraction within the temperature region of interest.

We show the T-x phase diagram of $Cu_{1-x}Mg_xGeO_3$ in Fig. 5. We have added T'_{SP} as closed diamonds and T_{SP} determined by the neutron diffraction[13] as plusses there. The T'_{SP} decreases with x and vanishes at $x_c \sim 0.024$, i.e., the peak width does not tend to the resolution limit at low temperatures in the $x > x_c$ region.
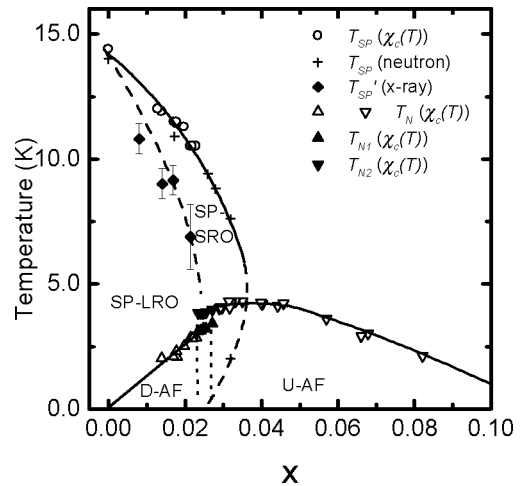

FIG. 5. T-x phase diagram of $Cu_{1-x}Mg_xGeO_3$ obtained by susceptibility measurements, x-ray diffraction and neutron diffraction. Neutron-diffraction data is from Fig. 6 of Ref. 13.

IV. DISCUSSION

We find clear double peaks in $\chi_c(T)$ [Figs. 2(a) and 3] and a corresponding jump of T_N in the T-x phase diagram [Fig. 2(b) and the inset of Fig. 3] of $Cu_{1-x}M_xGeO_3$ in the region $x_{c1} < x < x_{c2}$. While the jump of T_N is the strongest evidence for the existence of a first-order phase transition between the DAF and UAF phases, the double peaks suggest the existence of spatial phase separation at a critical concentration, which is characteristic of a first-order phase transition. The measured phase separation region spreads over a finite region, $x_{c1} < x < x_{c2}$, which is consistent with the phase transition being of the first order. When a first-order phase transition occurs, metastable phenomena, e.g., supercooling and superheating, appear around the critical point in general. The spread of the phase separation region over some nonzero range suggests the existence of metastable states as is indeed observed in the x-ray measurements.[11] We should note that this spread does not come from inhomogeneity of the impurity distribution in the case of Mg-doped $CuGeO_3$, because the concentration fluctuation is within 0.1% as shown in Fig. 1.

The fact that T'_{SP} is much lower than T_{SP} gives significant insight into how the SP order collapses with increasing impurity concentration. T_{SP} is the transition temperature inferred from the dip in the magnetic susceptibility, the jump of the heat capacity, and the appearance of measurable diffraction intensity at the SP superlattice peak positions. The coincidence of SP transition temperatures T_{SP} in various measurements, suggests that the correlation length of the dimerization of ~ 500 Å, which corresponds to the resolution limit of the neutron diffraction, is sufficient for the opening of the SP energy gap. In contrast to the case of pure $CuGeO_3$ system where T_{SP} and T'_{SP} are the same,[14] the one-dimensional spin chain is cut at the impurity site in the $Cu_{1-x}M_xGeO_3$ system. For $T_{SP} > T > T'_{SP}$, the phase of dimerization is likely pinned at the impurity sites, which is similar to the strong pinning interactions between the impurities and magnetic solitons which was suggested in the incommensurate phase in $Cu_{1-x}(Zn, Ni)_xGeO_3$.[15] However, only local lattice rearrangements are needed to change the phase at an impurity site. As the temperature decreases and the interchain interactions and spin-phonon coupling favoring the SP state become relatively more important, the individual finite SP domains begin to correlate with each other over large distances, and at T'_{SP} LRO is finally established. This model which could yield either a tricritical point with its concomitant first-order phase transition or a more complicated reentrant scenario as in certain spin glass systems. This is discussed briefly in Refs. 11 and 16.

Therefore, for $T_{SP} > T > T'_{SP}$, the SP energy gap and the dimerization coexist though the lattice dimerization does not attain LRO. Considering that the peak width determined in x-ray-diffraction measurements decreases gradually with decreasing temperature and that there is no anomaly in the susceptibility, heat capacity, and neutron peak intensity at T'_{SP}, we cannot determine definitively whether the change from SP-SRO to SP-LRO is a true phase transition or a crossover. The important point is that T'_{SP}, the temperature where ξ is much longer than the average impurity distance, vanishes around x_c [Figs. 2(c) and 5]. The jump of T_N at

$x_{c1} < x < x_{c2}$ corresponds to the disappearance of SP-LRO, which is the evidence for the phase transition between the UAF and DAF phases by x-ray diffraction. When x is larger than x_c, SP-SRO is still present in the system. However, it should be considered as the result of critical fluctuations of the true SP state found for $x < x_c$.

Recently, Nakao et al.[13] have reported neutron-diffraction measurements performed on Mg-doped $CuGeO_3$ crystals. This group of authors, which included some of the present authors, deduced the existence of the phase boundary between the DAF and UAF phases from the sudden change in SP lattice displacement δ and effective magnetic moment μ_{eff} at x_c. They have also proposed the existence of an intermediate phase with SP-SRO which is reentrant at low temperatures, and the existence of a phase transition between the DAF and UAF phases at $T = 0$ K. This reentrancy has also been clearly seen in recent low-temperature synchrotron x-ray measurements.[16]

While some of the extant theories provide a qualitative description of how impurity doping suppresses the SP phase and how the AF phase is induced,[17,18] they fail to explain the transition between the DAF and UAF phases reported in our paper. Saito[10] has recently proposed a model for the phase transition between the DAF and UAF phases at $T = 0$ K, and very recently she showed that the order of the phase transition depends on the ratio between the spin-lattice coupling and the interchain interaction.[19] According to her work, the phase transition between the DAF and UAF phases can be of first order in the case of relatively large interchain interaction.

While a detailed theoretical description of the two different AF phases at nonzero temperatures is still absent, the behavior of T_N as a function of x can be qualitatively explained as follows. The one-dimensionality of the spin interaction in $CuGeO_3$ appears not to be as good[20] as that of conventional organic SP materials.[21] The T-x phase diagram of $CuGeO_3$ therefore would be that of a typical diluted antiferromagnet, i.e., a monotonic decrease of T_N with x would be observed, if the SP transition had not occurred in $CuGeO_3$. Actually, the occurrence of the SP phase suppresses the AF phase completely in pure $CuGeO_3$. As x increases, the SP phase is suppressed and the DAF phase develops at an infinitesimally small impurity concentration,[22] and at x_c the SP-LRO disappears and the phase transition from the DAF to UAF phase occurs. Since the SP-SRO, however, still exists above x_c, the AF phase is suppressed, and T_N exhibits a plateau for $x_c < x \lesssim 0.04$. For $x \gtrsim 0.04$ any SP-SRO is very weak (Ref. 13) and therefore typical behavior of a diluted antiferromagnet, that is, a monotonic decrease of T_N with x, is observed.

V. CONCLUDING REMARKS

We have confirmed the phase transition between the UAF and DAF phases in Mg-doped $CuGeO_3$ by detailed susceptibility measurements and high-resolution synchrotron x-ray-diffraction studies. The results of previous neutron-diffraction experiments also suggested a similar phase

transition. We found clear double peaks in the magnetic susceptibility around $x \sim x_c$. We have interpreted these peaks as the result of two separate Néel transitions, in which case spatial phase separation between the DAF and UAF phases is present in the system. These features are interpreted as the result of an intrinsic first-order transition.

Our x-ray-diffraction measurements show that the SP dimerization attains long-range order only for $x < x_c$. Thus the transition from the DAF to UAF phase is characterized by the loss of the SP long-range order.

Our susceptibility measurements show that $Cu_{1-x}Zn_xGeO_3$ exhibits the same kind of behavior as $Cu_{1-x}Mg_xGeO_3$, and the T-x phase diagrams of these compounds are very similar. We therefore conclude that the DAF and UAF phases, and the corresponding transition between these phases at x_c, are also present in Zn-doped $CuGeO_3$.

*Electronic address: tmasuda@ap.t.u-tokyo.ac.jp

†Also at Department of Advanced Materials Science, The University of Tokyo, 6th Engineering Bldg., 7-3-1 Hongo, Bunkyo-ku, Tokyo 113-8656, Japan.

‡Present address: Central Research Institute of Electric Power Industry, Komae, Tokyo 201-8511, Japan.

[1] M. Hase, I. Terasaki, and K. Uchinokura, Phys. Rev. Lett. **70**, 3651 (1993).

[2] M. Hase, I. Terasaki, Y. Sasago, K. Uchinokura, and H. Obara, Phys. Rev. Lett. **71**, 4059 (1993).

[3] S.B. Oseroff, S.-W. Cheong, B. Aktas, M.F. Hundley, Z. Fisk, and L.W. Rupp, Jr., Phys. Rev. Lett. **74**, 1450 (1995).

[4] M. Hase, N. Koide, K. Manabe, Y. Sasago, and K. Uchinokura, Physica B **215**, 164 (1995).

[5] L.P. Regnault, J.P. Renard, G. Dhalenne, and A. Revcolevschi, Europhys. Lett. **32**, 579 (1995).

[6] Y. Sasago, N. Koide, K. Uchinokura, M.C. Martin, M. Hase, K. Hirota, and G. Shirane, Phys. Rev. B **54**, R6835 (1996).

[7] M.C. Martin, M. Hase, K. Hirota, G. Shirane, Y. Sasago, N. Koide, and K. Uchinokura, Phys. Rev. B **56**, 3173 (1997).

[8] H. Fukuyama, T. Tanimoto, and M. Saito, J. Phys. Soc. Jpn. **65**, 1182 (1996).

[9] T. Masuda, A. Fujioka, Y. Uchiyama, I. Tsukada, and K. Uchinokura, Phys. Rev. Lett. **80**, 4566 (1998).

[10] M. Saito, J. Phys. Soc. Jpn. **67**, 2477 (1998).

[11] Y.J. Wang, V. Kiryukhin, R.J. Birgeneau, T. Masuda, I. Tsukada, and K. Uchinokura, Phys. Rev. Lett. **83**, 1676 (1999).

[12] M.E. Fisher, Philos. Mag. **7**, 1731 (1962).

[13] H. Nakao, M. Nishi, Y. Fujii, T. Masuda, I. Tsukada, K. Uchinokura, K. Hirota, and G. Shirane, J. Phys. Soc. Jpn. **68**, 3662 (1999). They determined the boundary of SP phase by the contour of the order parameter. The SP-SRO is suppressed quite strongly below T_N in the $x > x_c$ region and therefore the reentrant nature of SP-SRO was observed.

[14] Q.J. Harris, Q. Feng, R.J. Birgeneau, K. Hirota, G. Shirane, M. Hase, and K. Uchinokura, Phys. Rev. B **52**, 15 420 (1995).

[15] V. Kiryukhin, B. Keimer, J.P. Hill, S.M. Coad, and D.McK. Paul, Phys. Rev. B **54**, 7269 (1996).

[16] V. Kiryukhin, Y.J. Wang, S.C. LaMarra, R.J. Birgeneau, T. Masuda, I. Tsukada, and K. Uchinokura, cond-mat/9908369, Phys. Rev. B (to be published 1 April 2000).

[17] M. Mostovoy, D. Khomskii, and J. Knoester, Phys. Rev. B **58**, 8190 (1998).

[18] M. Fabrizio, R. Mélin, and J. Souletie, cond-mat/9807093 (unpublished).

[19] M. Saito (unpublished).

[20] M. Nishi, O. Fujita, and J. Akimitsu, Phys. Rev. B **50**, 6508 (1994).

[21] J.W. Bray, H.R. Hart, Jr., L.V. Interrante, I.S. Jacobs, J.S. Kasper, G.D. Watkins, and S.H. Wee, Phys. Rev. Lett. **35**, 744 (1975).

[22] This was shown experimentally in $Cu_{1-x}Zn_xGeO_3$ [K. Manabe, H. Ishimoto, N. Koide, Y. Sasago, and K. Uchinokura, Phys. Rev. B **58**, R575 (1998)].